Table S1. Kinetic parameters derived from fits to the heme trafficking data using Equation 2. The values indicated represent the mean ± SD of independent triplicate cultures. *p<0.05, **p<0.01, ***p<0.001 by one-way ANOVA with Dunnett's post-hoc test. Red asterisks indicate statistical significance relative to the cytosol within a given strain. Black asterisks indicate statistical significance relative to the WT strain of a given compartment.

Journal of Cell Science • Supplementary information

Table S1.

Strain	Location	$t_{1/2}$ (min)	k (min^{-1})	Amplitude (% Bound)	Lag Time (min)	Figure	Goodness of Fit (R^2)
WT	Cyt Nuc Mito	86(4) 75(3)* 89(4)	.032(.003) .041(.002)* .034(.003)	93(5) 87(4) 88(5)	24(4) 26(3) 29(4)	Fig. 2e	.9908 .9851 .9942
*hem1*Δ + ALA	Cyt Nuc Mito	171(7) 150(2)*** 173(9)	.030(.003) .059(.005)*** .028(.004)	86(7) 108(5)* 75(8)	104(7) 113(2) 102(9)	Fig. 3a	.9596 .9739 .9445
WT	Cyt Nuc Mito	92(2) 84(3)* 93(2)	.033(.001) .039(.002)* .033(.002)	75(5) 91(6)* 75(4)	31(2) 33(3) 32(2)	Fig. 5a	.9926 .9724 .9914
*mgm1*Δ	Cyt Nuc Mito	90(4) 42(9)***/*** 85(5)	.034(.002) .02(.01) .037(.003)	74(6) 27(5)***/*** 77(6)	31(4) 20(5)*/* 31(5)	Fig. 5a	.9901 .5293 .9908
WT	Cyt Nuc Mito	97(3) 82(4)* 99(3)	.033(.002) .041(.001)* .034(.003)	85(6) 105(5)* 82(4)	36(3) 33(4) 40(3)	Fig. 5c	.9805 .9779 .9668
rho^0	Cyt Nuc Mito	85(2) 77(2)* 96(3)	.035(.002) .044(.003)* .034(.002)	98(5) 99(4) 93(5)	27(2) 31(2) 37(3)	Fig. 5c	.9797 .9768 .9795
WT	Cyt Nuc Mito	87(2) 78(3)* 93(3)	.033(.002) .042(.002)* .030(.002)	80(4) 100(6)* 78(4)	26(2) 30(3) 26(3)	Fig. 5e	.9854 .9692 .9783
*fzo1*Δ	Cyt Nuc Mito	89(2) 79(2)* 89(2)	.033(.002) .039(.002)* .032(.002)	87(5) 95(4) 90(4)	28(2) 28(2) 27(2)	Fig. 5e	.9888 .9805 .9897
WT	Cyt Nuc Mito	85(3) 75(2)* 87(2)	.031(.001) .041(.002)* .031(.002)	87(4) 94(5) 75(3)	20(3) 26(2) 22(2)	Fig. 5g	.9908 .9840 .9867
*ugo1*Δ	Cyt Nuc Mito	100(4) 77(3)* 96(3)	.028(.003) .039(.002)* .028(.001)	95(4) 102(6) 96(4)	28(4) 25(3) 25(3)	Fig. 5g	.9924 .9854 .9906
WT	Cyt Nuc Mito	89(2) 75(2)* 92(2)	.030(.002) .041(.002)* .032(.002)	88(4) 105(5)* 83(4)	22(2) 26(3) 28(2)	Fig. 5i	.9889 .9873 .9824
*pcp1*Δ	Cyt Nuc Mito	85(2) 69(3)* 90(3)	.033(.002) .045(.003)* .034(.001)	90(4) 105(6) 86(5)	24(2) 24(3) 31(3)	Fig. 5i	.9872 .9898 .9859
WT	Cyt Nuc Mito	119(3) 110(4) 111(3)	.033(.003) .041(.003)* .033(.002)	78(5) 96(5)* 80(4)	58(3) 61(4) 50(3)	Fig. 5k	.9886 .9488 .9767
*mic60*Δ	Cyt Nuc Mito	114(3) 104(3) 114(2)	.033(.003) .039(.003)* .031(.002)	78(6) 96(5)* 81(4)	54(3) 53(3) 50(2)	Fig. 5k	.9874 .9686 .9876
WT	Cyt Nuc Mito	102(3) 88(4)* 99(4)	.030(.002) .038(.002)* .031(.001)	80(4) 85(6) 75(5)	35(3) 35(4) 34(4)	Fig. 6a	.9833 .9449 .9778
*dnm1*Δ	Cyt Nuc Mito	80(2) 64(2)*/* 82(2)	.038(.002)* .055(.003)**** .036(.002)*	93(4) 105(5)* 93(3)	27(2) 27(2) 26(2)	Fig. 6a	.9874 .9669 .9885
WT	Cyt Nuc Mito	86(2) 75(3)* 89(2)	.032(.002) .042(.003)* .033(.002)	87(3) 93(4) 84(3)	24(2) 27(3) 28(2)	Fig. 6c	.9876 .9827 .9931
*fis1*Δ	Cyt Nuc Mito	92(2) 83(3)* 95(3)	.032(.002) .040(.001)* .032(.002)	84(3) 95(5) 80(4)	30(2) 33(3) 32(3)	Fig. 6c	.9898 .9714 .9820

Journal of Cell Science • Supplementary information

WT	Cyt	132(7)	.018(.002)	80(4)	21(7)	Fig. 6e	.9756
	Nuc	78(2)*	.035(.002)***	107(5)*	21(2)		.9800
	Mito	115(10)	.021(.001)	90(3)	20(10)		.9880
caf4Δ mdv1Δ	Cyt	144(9)	.017(.002)	79(5)	26(9)	Fig. 6e	.9836
	Nuc	81(4)*	.031(.002)***	104(6)*	17(4)		.9754
	Mito	137(4)	.020(.001)	95(6)*	37(4)		.9887
WT	Nuc	114(5)	.034(.005)	60(5)	55(5)	Fig. 6g	.9599
dnm1Δ	Nuc	100(7)*	.050(.003)**	103(7)**	57(7)	Fig. 6g	.9439
mgm1Δ	Nuc	82(4)*	.010(.004)**	26(3)***	48(4)	Fig. 6g	.6445
dnm1Δ mgm1Δ	Nuc	99(5)	.032(.003)	69(4)	36(5)	Fig. 6g	.9402
WT	Cyt	95(3)	.031(.002)	80(4)	34(3)	Fig. 4a	.9814
	Nuc	88(4)*/*	.041(.003)*	90(3)	37(4)		.9403
	Mito	93(3)	.032(.002)	87(3)	31(3)		.9833
gem1Δ	Cyt	87(4)	.031(.001)	86(3)	21(4)	Fig. 4a	.9890
	Nuc	61(4)**/**	.051(.002)**/*	104(5)*	17(4)		.9753
	Mito	93(3)	.033(.002)	77(6)	30(3)		.9837
WT	Cyt	99(3)	.031(.002)	81(3)	35(3)	Fig. 4c	.9724
	Nuc	89(4)*	.039(.003)*	93(3)*	37(4)		.9580
	Mito	96(4)	.033(.002)	79(3)	35(4)		.9696
mdm12Δ	Cyt	113(4)	.028(.002)	84(3)	41(4)	Fig. 4c	.9830
	Nuc	101(5)	.035(.002)*	100(5)*	43(5)		.9481
	Mito	109(4)	.029(.003)	70(3)	40(4)		.9669
WT	Cyt	33(3)	.029(.001)	91(3)	0	Fig. 4e	.9947
	Nuc	19(3)**	.045(.002)**	106(5)*	0		.9775
	Mito	35(4)	.031(.002)	91(3)	0		.9873
mdm34Δ	Cyt	50(5)	.024(.003)	93(4)	0	Fig. 4e	.9943
	Nuc	22(3)	.040(.004)**	106(4)*	0		.9678
	Mito	43(4)	.024(.002)	105(5)	0		.9841
WT	Cyt	154(5)	.018(.001)	80(5)	43(5)	Fig. 4g	.9871
	Nuc	115(3)***	.030(.003)***	85(4)	48(3)		.9921
	Mito	145(6)	.020(.002)	82(4)	45(6)		.9808
psd1Δ	Cyt	156(3)	.019(.001)	80(3)	50(3)	Fig. 4g	.9826
	Nuc	106(5)***	.033(.003)***	82(4)	45(5)		.9863
	Mito	145(4)	.023(.003)	84(3)	55(4)		.9891
WT	Cyt	83(4)	.031(.002)	90(3)	19(4)	Fig. 4i	.9860
	Nuc	67(3)	.039(.002)*	98(4)	16(3)		.9738
	Mito	86(3)	.032(.003)	90(2)	24(3)		.9781
ypt7Δ	Cyt	100(4)	.032(.002)	99(3)	38(4)	Fig. 4i	.9791
	Nuc	94(3)	.038(.002)*	100(4)	42(3)		.9172
	Mito	101(3)	.029(.003)	92(5)	32(3)		.9206
WT	Cyt	67(2)	.031(.002)	88(4)	3(2)	Fig. 4k	.9867
	Nuc	59(2)*	.038(.002)*	105(6)*	6(2)		.9748
	Mito	65(3)	.029(.003)	85(3)	1(3)		.9791
vps39Δ	Cyt	75(3)	.029(.003)	95(3)	6(3)	Fig. 4k	.9836
	Nuc	64(4)*	.039(.002)**	104(5)	13(4)		.9490
	Mito	81(4)	.027(.002)	103(5)	7(4)		.9699

Fig. S1. Related to Fig. 2. A 500 µM dose of succinylacetone (SA) depletes (**a**) total heme and (**b**) heme-loading of the heme sensor, HS1, to values similar to heme deficient *hem1*Δ cells, which lack the 1st enzyme in the heme biosynthetic pathway. Moreover, the expression of cytosolic, nuclear, and mitochondrial HS1 do not affect steady-state cellular heme content. All data represent the mean ± SD of triplicate cultures.

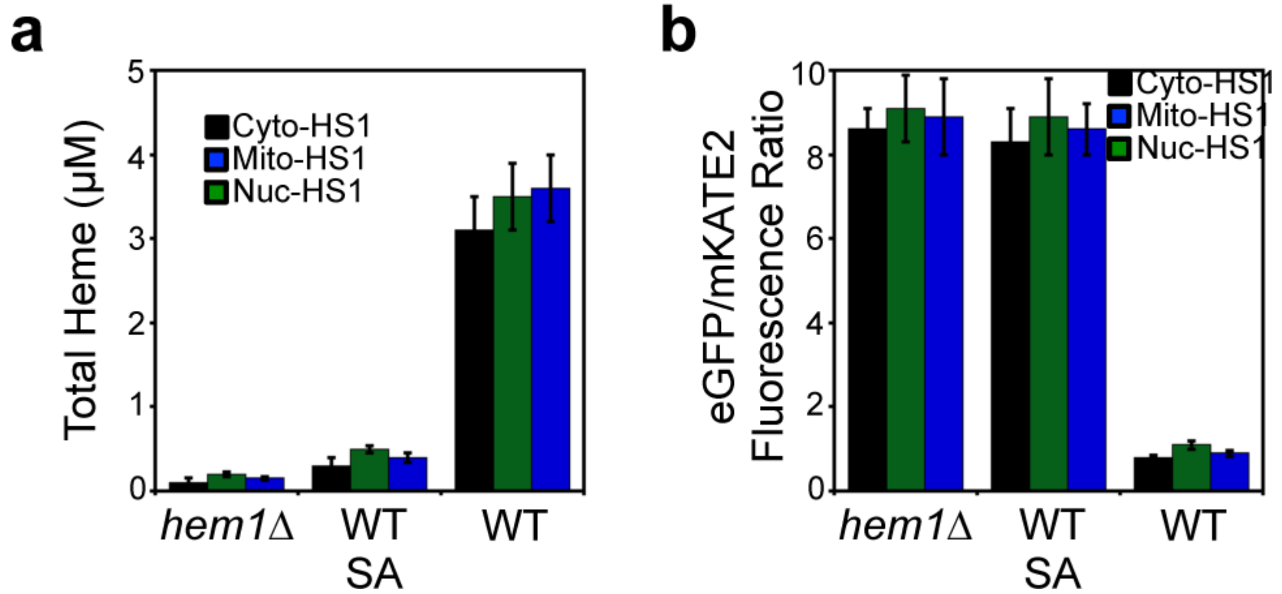

Fig. S2. Related to Fig. 2. Heme sensor expression in the indicated compartments do not perturb (**a**) the rates of heme synthesis or (**b**) heme trafficking dynamics to the cytosol. (**a**) WT cells expressing *GPD* driven cytosolic (Cyto, black), mitochondrial (Mito, blue), or nuclear (Nuc, green) HS1, or empty vector (EV, grey) were heme depleted with 500 μM succinylacetone (SA) for 15 hours and then the cells were resuspended in fresh SC-LEU media lacking SA, where the re-synthesis of heme was monitored by harvesting 2 x 10^8 cells every hour and analyzed for heme content as decribed in the **Method Details**. (**b**) The heme trafficking dynamics assay was conducted on cells expressing *ADH* (black), *TEF* (green) and *GPD* (blue) driven cytosolic HS1. Despite the ~10-fold increase in HS1 expression between *ADH* and *GPD* promoters, as measured by mKATE2 fluorescence in the right panel (**c**), cytosolic heme trafficking rates are virtually identical. All data represent the mean ± SD of triplicate cultures.

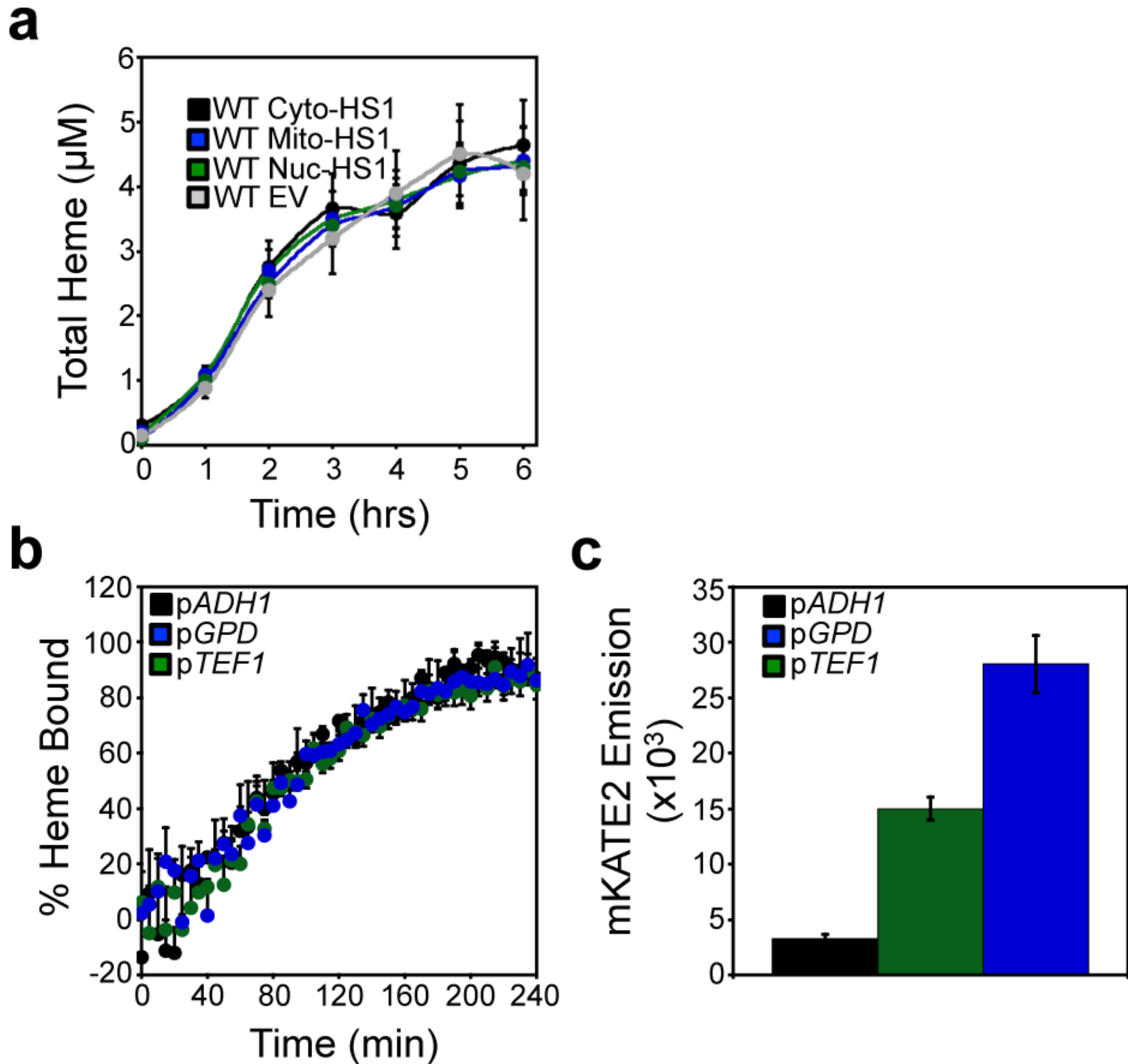

Journal of Cell Science • Supplementary information

Fig. S3. Related to Fig. 2. Heme binding kinetics of cytosolic, nuclear, and mitochondrial-targeted HS1. 2 x 10^8 exponential-phase WT cells expressing *GPD* driven cytosolic (Cyto, black), mitochondrial (Mito, blue), or nuclear (Nuc, green) HS1 were lysed in 500 µL of PBS buffer containing 10 mM ascorbate and 0.1% Triton X-100. 100 uL of the cell lysate was analyzed by fluorescence (ex. 488 nm, em. 510 nm; ex. 588 nm, em. 620 nm) over the indicated time period, and at time 0, an automatic dispenser pipetted 5 µL of a 1 mM hemin chloride stock solution in DMSO, giving a final concentration of 50 µM heme in the cell lysate. All data represent the mean ± SD of triplicate cultures.

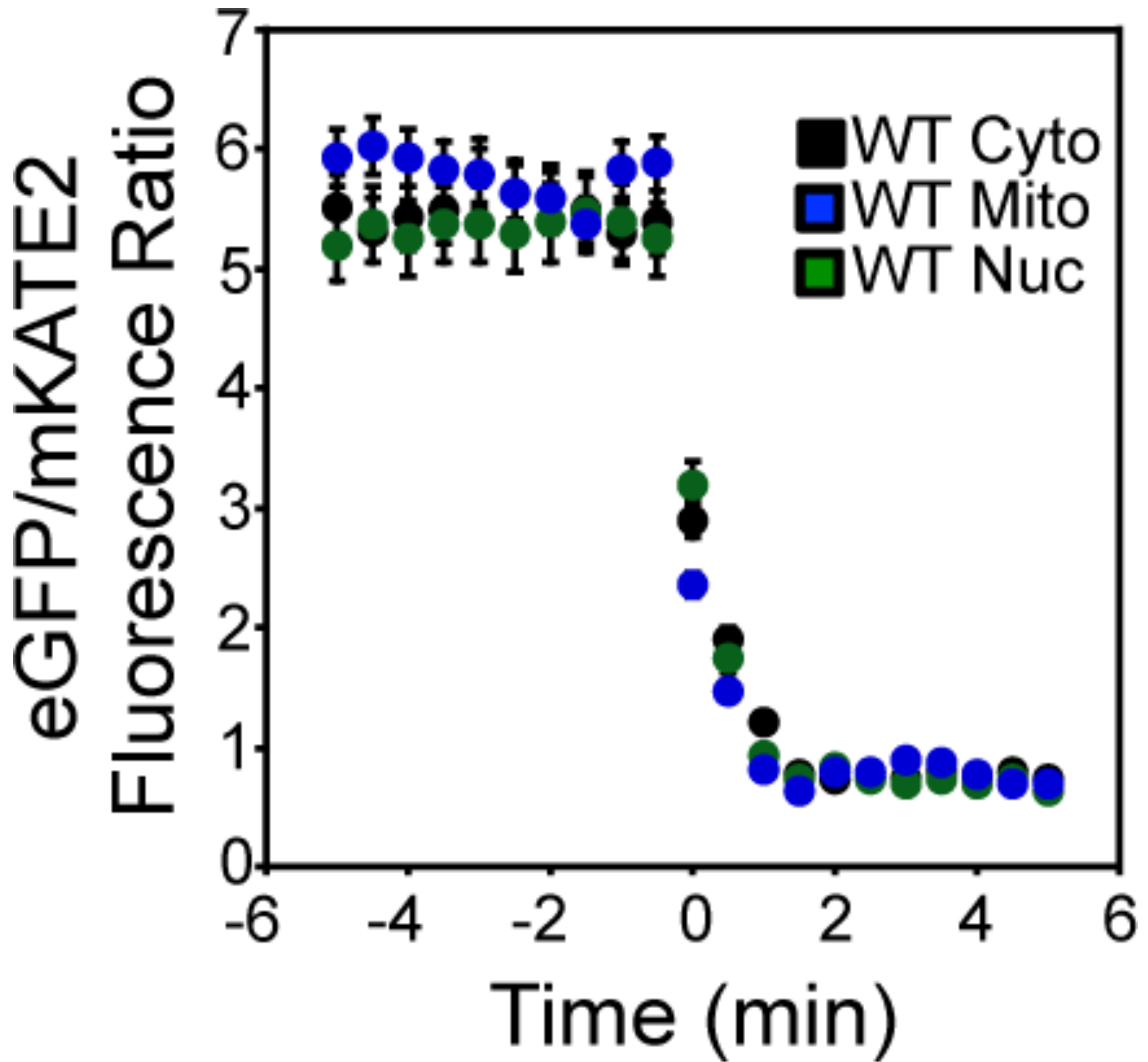

Fig. S4. Related to Fig. 5 and Fig. 6. The effects of *mgm1*Δ and *dnm1*Δ on steady-state HS1 heme loading and heme synthesis. (**a**) Cytosolic (Cyto), nuclear (Nuc), or mitochondrial (Mito) HS1 expressed in WT (black, gray), *dnm1*Δ (dark and light green), and *mgm1*Δ (dark and light blue) cells were cultured for 16 hours in SCE-LEU media with (+SA, dark colors) or without (-SA, light colors) 500 µM succinylacetone (SA). Following growth and washing cells with ultrapure water, HS1 sensor fluorescence was measured in a 100 µL suspension of 5 OD's/mL in PBS. (**b and c**) The rates of heme synthesis were measured in (**b**) *mgm1*Δ and (**c**) *dnm1*Δ cells by first heme depleting cells with 500 µM SA for 15 hours and then re-initiating heme synthesis by re-suspending cells in media lacking SA. 2 x 10^8 cells were harvested every hour and analyzed for heme content as described in the **Materials and Methods**. All data represent the mean ± SD of triplicate cultures.

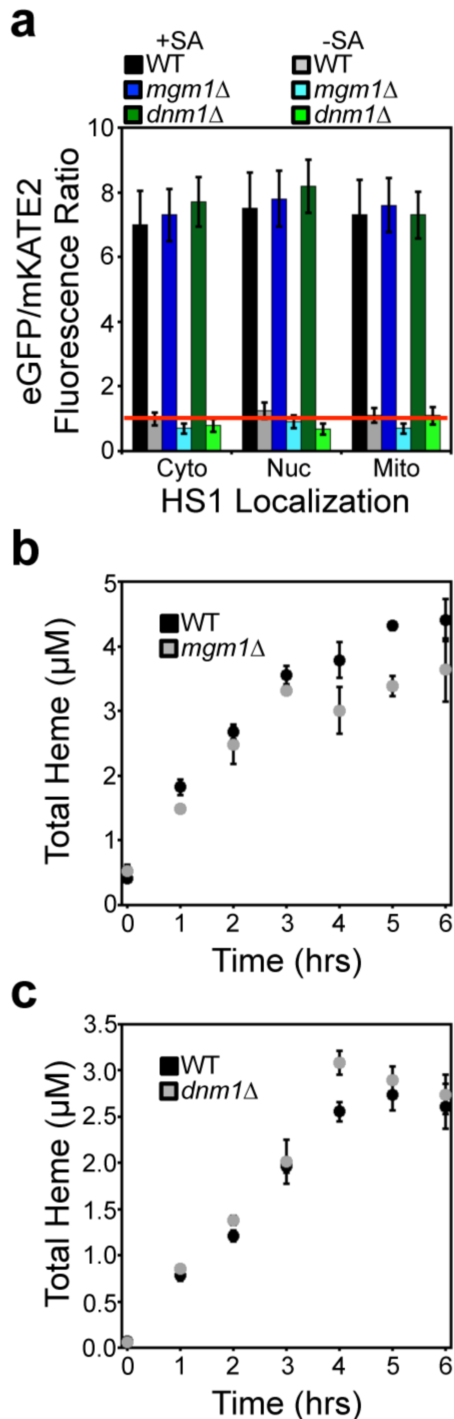

Journal of Cell Science • Supplementary information

Fig. S5. Related to strain validation in Materials and Methods. Validation of the mitochondrial network morphology defects in yeast fission and fusion mutants. (**a**) Sampling and classification of mitochondrial network morphologies observed using Mitotracker staining of cells. (**b**) Histograms of mitochondrial network morphology in the fission and fusion mutants used throughout this study. Mutants defective in mitochondrial fission exhibit an elongated mitochondrial network. Mutants defective in mitochondrial fusion exhibit a punctate mitochondrial network. WT and *mgm1*Δ *dnm1*Δ cells tend to have a more equal distribution of elongated and punctate mitochondrial networks. The histograms were generated by analyzing ~50 cells per mutant. (**c**) Representative images of the mitochondrial network in the fission and fusion mutants utilized in this study. Scale bar: 5.0 um.

Journal of Cell Science • Supplementary information

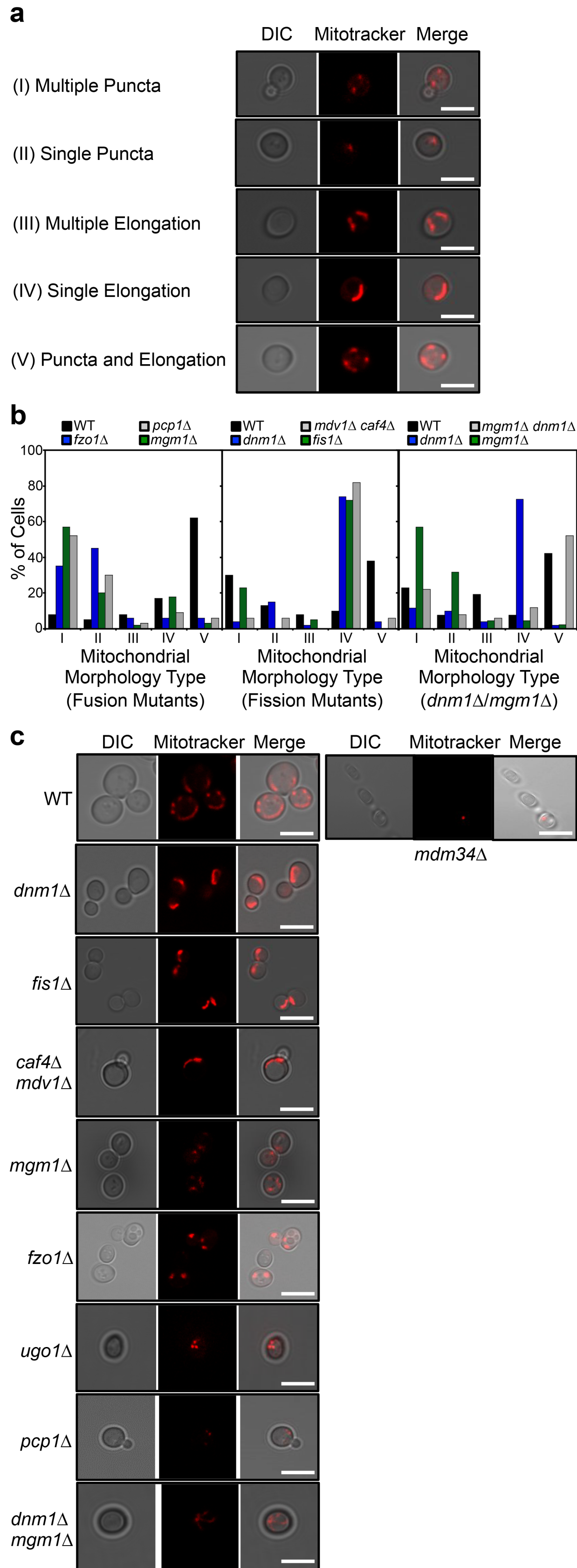

Journal of Cell Science • Supplementary information